Mem. S.A.It. Vol. 88, 54
© SAIt 2017
Memorie della

On the effect of vorticity on the propagation of internal gravity waves

G. Vigeesh[1], O. Steiner[1,2], F. Calvo[2], and M. Roth[1]

[1] Kiepenheuer-Institut für Sonnenphysik, Schöneckstrasse 6, 79104 Freiburg, Germany
e-mail: vigeesh@leibniz-kis.de
[2] Istituto Ricerche Solari Locarno (IRSOL), via Patocchi 57–Prato Pernice, 6605 Locarno-Monti, Switzerland

Abstract. We compare different models of solar surface convection to study vorticity and how it can influence the propagation of internal gravity waves. We conclude that simulations performed with higher grid resolution may have a reduced gravity wave flux in the lower part of the atmosphere due to strong vorticity. We also show that the vertical extent of the allowed region of propagation depends on the magnetic field inclination.

Key words. Magnetohydrodynamics (MHD) – Methods: numerical – Convection –Sun: atmosphere – Sun: magnetic fields – Sun: waves

1. Introduction

The CO5BOLD code (Freytag et al. 2012) has been employed for numerous astrophysical applications, including the study of wave phenomena in the solar atmosphere. The outstanding stability and robustness of the code allows to compute long time periods of solar/stellar magneto-convection. This has made it a great tool to study waves that are naturally excited and are propagating in a dynamically evolving (magneto-)atmosphere.

In a recent paper, we carried out an investigation of the acoustic-gravity wave spectrum emerging from a realistic numerical simulation of the solar near-surface layers, performed using the CO5BOLD code (Vigeesh et al. 2017). Our main focus was on internal gravity waves (IGWs) in the Sun's atmosphere, motivated by the work of Straus et al. (2008). Using non-magnetic CO5BOLD simulations and observations, Straus et al. (2008) showed that these waves carry enough energy to balance the radiative losses of the entire chromosphere. We extended their work by including magnetic fields and studying its effect on the propagation of IGWs.

Summarizing the main result of our paper, we found that the IGWs are absent or partially reflected back into the lower layers when there are vertical magnetic fields present in the atmosphere. Mode-conversion of IGWs to slow magneto-acoustic waves was found to be a principle reason for this. Although not completely evident in our analysis, we argued that vorticity may also influence the propagation of IGWs.

IGWs are waves propagating in a stably stratified fluid as a result of a perturbation to its equilibrium state, with buoyancy acting as the restoring force. In the solar atmosphere, IGWs are thought to be generated by material overshooting from the convection zone into the stably stratified atmosphere above. Once generated, the propagation of these waves in the atmosphere is affected by several factors, the presence of a strong background flow being one of them. Whenever an IGW encounters a region where the horizontal phase speed of the wave becomes equal to the mean flow, the region acts as a "critical level", resulting in the absorption/reflection or breaking of these waves (see e.g., Sutherland 2010). We suggest that the presence of strong vorticity can provide such a condition for IGWs in the solar atmosphere.

Vortex flows are ubiquitously present in the photosphere and chromosphere (Brandt et al. 1988; Bonet et al. 2008, 2010; Wedemeyer-Böhm & Rouppe van der Voort 2009; Steiner et al. 2010; Vargas Domínguez et al. 2011). These vortical motions are typically associated with the convective downdrafts at the boundaries of granules in the photosphere and with magnetic fields in the chromosphere. Vortices have also been studied in numerical simulations of magneto-convection (Muthsam et al. 2010; Moll et al. 2011; Kitiashvili et al. 2011; Shelyag et al. 2011; Steiner & Rezaei 2012), and have been found to be prominent on much smaller spatial scales than the granulation.

While carrying out the analysis for Vigeesh et al. (2017), we found that fluid vorticity in the presence of magnetic fields increases more steeply with height compared to a non-magnetic model. However, the magnitude of the vorticity, in both cases, was found to be not significant enough to influence the propagation of IGWs. The fact that we used a coarse resolution simulation might have had an impact on our analysis. In this paper, we look at different models of solar surface convection and their ability to capture strong vorticity. We see that, performing a high resolution simulation may have a significant impact on IGWs that are generated in the models.

2. Numerical models

The models studied in this work were computed using two different versions of the `CO5BOLD` code. We started with an earlier version (`002.00.2011.04.28`) to compute a low-resolution ($\delta x, \delta y = 80$ km), non-magnetic model and a magnetic model with initially uniform vertical fields. The non-magnetic model was computed using the Roe solver (roe) with VanLeer reconstruction and the magnetic model was computed with a HLLMHD solver with PP/VanLeer reconstruction (Steiner et al. 2013). The fact that the HLLMHD solver is more diffusive compared to the Roe solver resulted in larger granules in the magnetic model. Nevertheless, these two models were compared with respect to the internal gravity wave spectrum emerging out of the surface convection. The analysis by which the waves are detected and the main results of this study has been reported in Vigeesh et al. (2017).

In order to ascertain that the internal gravity wave spectrum is unaffected by the choice of the solver, we have now computed another set of models with the same solver for the non-magnetic and magnetic models. For this we use the newer version (`002.02.2012.11.05f`) of `CO5BOLD`. The "non-magnetic" model was computed by setting the initial magnetic field $\boldsymbol{B} = 0$ G (b0). Another set of two magnetic models, one with an initial vertical field $B_z = 50$ G (v50) and another with an initial horizontal field with $B_x = 50$ G (uh50) have also been computed. These models will be further used for the study of IGWs to better understand the mode-conversion scenario, with the focus on its dependence on the magnetic field inclination.

The main drawback of the aforementioned low-resolution simulations are that they do not capture strong vorticity. This results in the misrepresentation of their importance in the study of IGWs. Therefore, we thought that it would be worthwhile to look at simulations that capture strong vorticity and to estimate their influence on the propagation properties of IGWs. For this purpose, we have used another set of high-resolution simulations ($\delta x, \delta y = 10$ km) from F. Calvo (see also Steiner et al. 2017, this volume). We analysed snapshots from four sets of simulations, two non-magnetic (computed with the Roe and HLLMHD solver) and two magnetic models (computed with the HLLMHD solver with initially vertical (v50)

Table 1. Numerical setup and physical properties of the representative snapshots. The rms bolometric intensity contrast refers to the single snapshot analyzed in this work.

	High-resolution				Low-resolution			
	roe	b0	v50	h50	roe	b0	v50	uh50
Comp. grid	960×960×280				480×480×120			
Domain size (Mm^3)	9.6×9.6×2.8				38.4×38.4×2.8			
Comp. cell size (km^3)	10×10×10				80×80×(50-20)			
Numerical scheme	Roe	⟵ HLLMHD ⟶			Roe	⟵ HLLMHD ⟶		
Reconstruction	⟵ FRweno ⟶				VanLeer	⟵ FRweno ⟶		
Int. contrast, $\delta I^{\mathrm{rms}}_{\mathrm{bol}}$ (%)	15.70	14.88	15.00	14.80	15.40	15.40	14.76	15.47

and horizontal fields (h50)). The models compared in this paper are summarized in the Table 1.

The boundary conditions of all the models considered here are the same (with the exception of the boundary conditions for the magnetic field for high-resolution, h50). The velocity field, the radiation, and the magnetic field components are periodic in the lateral directions. The top boundary is open for fluid flow and outward radiation. The height (above $z_{\langle\tau_{\mathrm{R}}=1\rangle}$) and the depth (below $z_{\langle\tau_{\mathrm{R}}=1\rangle}$) of the box are around 1.3 and 1.5 Mm, respectively. The low-resolution models have a larger computational domain in horizontal scale (38.4 Mm), for the purpose of studying IGWs. The high-resolution models are smaller in horizontal size (9.8 Mm) and were not intended for wave studies. The main difference between the magnetic high-resolution (h50) and low-resolution (uh50) model is that the later was computed by imposing a uniform horizontal field of 50 G while in the former, horizontal field of strength $B_h = 50$ G is advected across the lower boundary into the box (for more details of this boundary condition see Steiner et al. 2008). For v50, the vertical component of the magnetic field is constant across the top and bottom boundaries and the transverse component is forced to vanish.

Figure 1 shows snapshots of the emerging bolometric intensity from the three high-resolution models (b0, v50, h50). Figure 2 shows snapshots of the emerging bolometric intensity from the three low-resolution models (b0, v50, uh50), with a zoomed-in field of view shown in the top panels, for the sake of comparison with the high-resolution runs.

3. Analysis

Internal gravity waves can only propagate below the Brunt-Väisälä frequency, N, defined as,

$$N^2 = g\left(\frac{1}{H_\varrho} - \frac{1}{\gamma H_{\mathrm{p}}}\right), \qquad (1)$$

where, γ is the ratio of the specific heats (c_P/c_V), H_ϱ is the density scale height, and H_{p} is the pressure scale height of the atmosphere. When these waves propagate in the presence of a background flow, their propagation properties are modified. In the context of IGWs, Mihalas & Toomre (1981) consider a stability condition given by the ratio of wave vorticity (ζ) and N to describe the importance of vorticity on IGWs.

For the purpose of the present analysis, we only look at individual snapshots taken from a set of simulations. Therefore, we look at the fluid vorticity ($\boldsymbol{\omega} \equiv \boldsymbol{\nabla} \times \boldsymbol{v}$) to get an estimate of its relevance for the IGW study, rather than going into the Fourier domain to calculate the wave vorticity (ζ). Vorticity does not necessarily mean that there are vortex flows in the model. Vorticity also occurs due to velocity shears, which appear to be present in the models presented here. A more detailed description of vortex flows is provided by the swirling

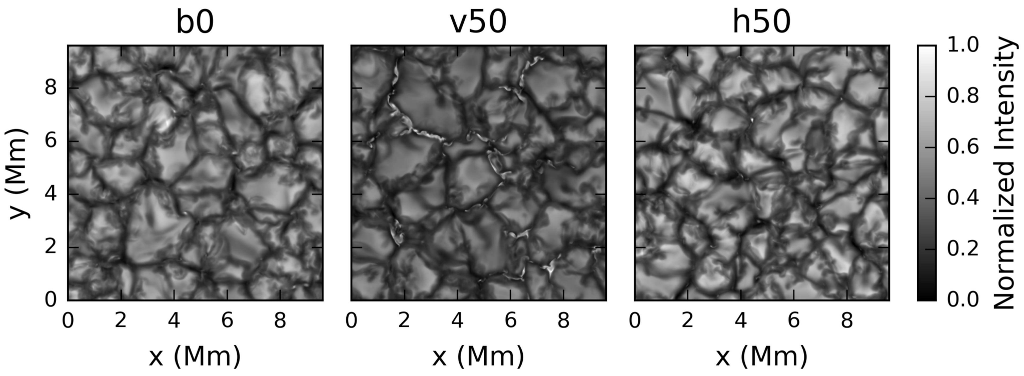

Fig. 1. Bolometric intensity emerging from the three high-resolution models. The grey-scale ranges from minimum (0) to maximum (1) intensity for each panel individually.

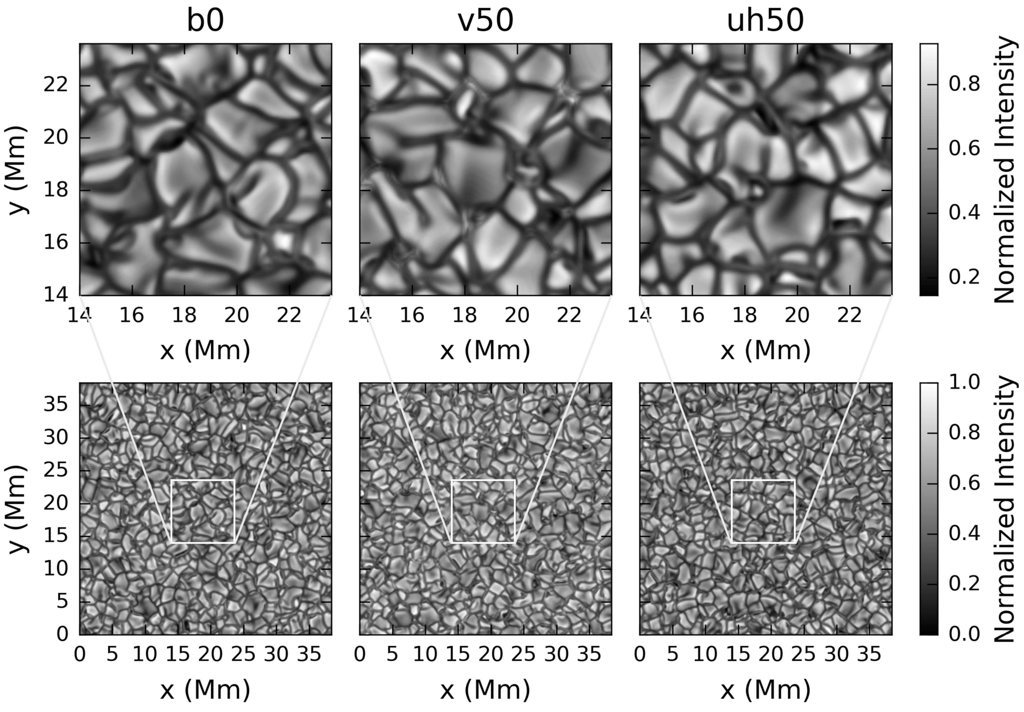

Fig. 2. Bolometric intensity emerging from the three low-resolution models. The *bottom panels* show the full box, and the *top panels* show the field of view corresponding to the size of the high-resolution runs shown in Fig. 1. The grey-scale range is defined in the same way as in Fig. 1

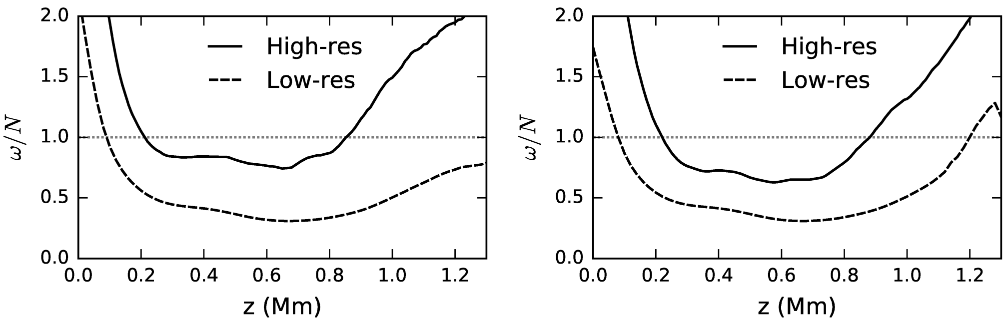

Fig. 3. Horizontally averaged ratio ω/N as a function of height from a single snapshot taken from the non-magnetic models. The *left panel* is from the models computed using the Roe solver (roe) and the *right panel* is from the models computed using the HLLMHD solver (b0). *Solid curves* in both panels refer to high-resolution ($\delta x, y = 10$ km) run and the *dashed curves* to the low-resolution ($\delta x, y = 80$ km) run.

strength (Moll et al. 2011), which we have not attempted here, as we are mainly interested in the internal gravity waves and how these waves are affected by shear.

4. Results

In the following, we show the ratio ω/N calculated from the different models described in Table 1.

4.1. Non-magnetic models

Figure 3 shows the horizontally averaged ratio ω/N as a function of height computed from a single snapshot taken from the non-magnetic models. The two sets of non-magnetic models that we compare here are computed using the hydrodynamic Roe solver (Fig. 3, left panel) and the magnetohydrodynamic HLLMHD solver by setting $B = 0$ (Fig. 3, right panel). We compare the high-resolution with the low-resolution run in each set. The model with high-resolution is shown by the solid curve and the low-resolution by the dashed curve. In all the runs, we see that ω/N is greater than 1 near the surface layers but drops below 1 as we go slightly higher up in the atmosphere. The ratio in the low-resolution model drops below 1 lower in the atmosphere ($\sim$100 km) when compared to the high-resolution runs, which show this drop only around 200 km. This indicates that the vorticity generated in the low-resolution runs are weak (relative to N) and IGWs can survive in the lower regions, which may not be the case with the high-resolution models.

Higher up in the atmosphere, we see a drastic difference between the high- and low-resolution runs. When using the Roe solver with low-resolution (Fig. 3, left panel), we see that ω/N is below 1 everywhere in the atmosphere, suggesting that the IGWs do not suffer any strong vorticity and can propagate unhindered. However, with the Roe solver in the high-resolution model, we see that the generated vorticities are strong such that IGWs cannot exist above 800 km, allowing them only in a restricted height range to propagate freely.

Now we look at the models computed using the HLLMHD solver shown in the right panel of Fig. 3. Vorticity in these models are remarkably similar to the vorticity in the models computed with the (less diffusive) Roe solver, even though we use here only one single snapshot, not a temporal mean. Looking at the low-resolution run (dashed curves), we see a slight increase in ω/N with height in the top part of the box, which is probably due to the usage of the less diffusive FRweno reconstruction scheme. Once again, the high-resolution model shows the same trend as we have seen with the Roe solver, suggesting that IGWs may be confined to a restricted height range due to the presence of strong vorticity.

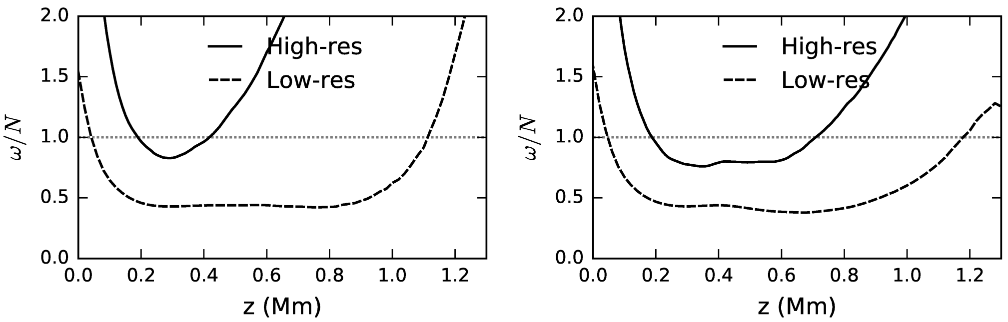

Fig. 4. Horizontally averaged ratio ω/N as a function of height from a single snapshot taken from the non-magnetic models. The *left panel* is from the models computed with the HLLMHD solver with an initial vertical magnetic field (v50) and the *right panel* is from model with initial horizontal fields (h50 and uh50). *Solid curves* in both panels refer to the high-resolution ($\delta x, y = 10$ km) runs and the *dashed curves* refer to the low-resolution ($\delta x, y = 80$ km) run.

4.2. Magnetic models

Figure 4 shows the horizontally averaged ratio ω/N as a function of height computed from a single snapshot taken from the magnetic models. The two sets of magnetic models are computed using the HLLMHD solver with an initial vertical field (Fig. 4, left panel) and an initial horizontal field (Fig. 4, right panel). The solid curves refer to the model with high-resolution and the dashed curves to the model with low-resolution. In the lower layers, the low-resolution model shows a drop of the ratio ω/N with height similar to that seen in the non-magnetic models discussed in Sect. 4.1. However, ω/N falls below 1 much deeper in the magnetic atmosphere than in the non-magnetic case, owing to the fact that the vorticities are weaker near the surface in the presence of magnetic fields. In the top part of the atmosphere, both v50 and uh50 show a similar trend in the low-resolution runs, allowing waves to propagate up to ~1.1 Mm in the atmosphere. However, the high-resolution runs show a major difference between the vertical and the horizontal initial field and are also markedly different from the low resolution runs. Having a vertical field is seen to confine the IGWs to a very small height range (200 - 400 km), whereas this height range is much broader in the case of initially horizontal fields (200 - 700 km). The strong vorticity in the upper layers of the model v50 is caused by magnetic fields whose footpoints are trapped in (quasi) rotative motions in the convective surface layers (Shelyag et al. 2011; Steiner & Rezaei 2012; Wedemeyer-Böhm et al. 2012).

5. Conclusions

We find that the vorticity is stronger in high-resolution compared to low-resolution runs and consequently, the ratio of vorticity to the Brunt-Väisälä frequency, ω/N, is greater, suggesting that vorticity may have a significant effect on the propagation of internal gravity waves (IGWs) generated in the solar atmosphere. We predict that a simulation performed with higher grid resolution than we have done so far may contain a reduced IGW flux in the lower part of the atmosphere. It can also restrict the spatial height range in which the IGWs can exist. We also find a dependence on the magnetic field inclination. Models with predominantly vertical fields confine IGWs to a smaller height range in the atmosphere than models with predominantly horizontal fields. With the high-resolution simulations, we always find a restricted range in height where IGWs can exist, reaffirming their existence in the real solar atmosphere. The analysis presented in this paper is only preliminary, in that we do not directly study the IGWs generated in the simulation. We would like to point out that, performing a high-resolution, large-box, long-duration simulation to study IGWs and the effect of vorticity on them is computationally expensive.

Acknowledgements. This work was supported by the German Research Foundation (DFG) grant RO 3010/3-1. The high-resolution simulations have been computed at the Swiss National Supercomputing Center (CSCS) under project ID s560. This work was supported by the Swiss National Science Foundation under grant ID 200020_157103/1.

References

Bonet, J. A., et al. 2008, ApJ, 687, L131
Bonet, J. A., Márquez, I., Sánchez Almeida, J., et al. 2010, ApJ, 723, L139
Brandt, P. N., et al. 1988, Nature, 335, 238
Freytag, B., Steffen, M., Ludwig, H.-G., et al. 2012, J. Comp. Phys., 231, 919
Kitiashvili, I. N., et al. 2011, ApJ, 727, L50
Mihalas, B. W. & Toomre, J. 1981, ApJ, 249, 349
Moll, R., Cameron, R. H., & Schüssler, M. 2011, A&A, 533, A126
Muthsam, H. J., Kupka, F., Löw-Baselli, B., et al. 2010, New Astron., 15, 460
Shelyag, S., et al. 2011, A&A, 526, A5
Steiner, O., et al. 2008, ApJ, 680, L85
Steiner, O., Franz, M., Bello González, N., et al. 2010, ApJ, 723, L180
Steiner, O. & Rezaei, R. 2012, in Fifth Hinode Science Meeting, ed. L. Golub, I. De Moortel, & T. Shimizu (ASP, San Francisco), ASP Conf. Ser., 3
Steiner, O., Rajaguru, S. P., Vigeesh, G., et al. 2013, MSAIS, 24, 100
Steiner, O., et al. 2017, MmSAI, 88, 37
Straus, T., Fleck, B., Jefferies, S. M., et al. 2008, ApJ, 681, L125
Sutherland, B. R. 2010, Internal Gravity Waves (Cambridge Univ. Press, Cambridge)
Vargas Domínguez, S., et al. 2011, MNRAS, 416, 148
Vigeesh, G., Jackiewicz, J., & Steiner, O. 2017, ApJ, 835, 148
Wedemeyer-Böhm, S. & Rouppe van der Voort, L. 2009, A&A, 507, L9
Wedemeyer-Böhm, S., Scullion, E., Steiner, O., et al. 2012, Nature, 486, 505